Surface Freezing in Binary Mixtures of Alkanes: New Phases and Phase Transitions

X. Z. Wu,[1,2] B. M. Ocko,[3] H. Tang,[4] E. B. Sirota,[5] S. K. Sinha,[5] and M. Deutsch[6]
[1]*Physics Department, Northern Illinois University, DeKalb, Illinois 60115*
[2]*Material Sciences Division, Argonne National Laboratory, Argonne, Illinois 60439*
[3]*Physics Department, Brookhaven National Laboratory, Upton, New York 11973*
[4]*Department of Materials Science and Engineering, University of Illinois, Urbana, Illinois 61801*
[5]*Exxon Research and Engineering Company, Route 22 East, Annandale, New Jersey 08801*
[6]*Physics Department, Bar Ilan University, Ramat Gan 52900, Israel*
(Received 8 February 1995)

Surface freezing of a crystalline monolayer has been observed at the free surface of liquid binary mixtures of normal alkanes by x-ray and surface tension measurements. Two dramatically different behaviors are found for the monolayer properties depending on Δn, the difference in the components' carbon numbers. For small Δn, the variation with temperature and concentration is continuous. For large Δn, the variation is discontinuous, exhibiting surface segregation and 2D structural phase transitions. A theory based on competition between entropic mixing and a repulsive interaction due to chain length mismatch accounts well for the observed phenomena.

PACS numbers: 68.10.–m, 61.25.Em, 64.70.Dv, 82.65.Dp

The reduced dimensionality at an interface has a strong influence on the phase behavior of matter and may induce phenomena not observed in the bulk [1]. Binary mixtures provide an additional degree of freedom which can lead to prewetting, surface enrichment, and surface layering [2], all studied extensively on macroscopic and mesoscopic scales. Angstrom-scale studies of binary mixture surfaces are very few. The recently discovered surface freezing of a crystalline monolayer at the liquid/vapor interface of n alkanes [$CH_3(CH_2)_{n-2}CH_3$, or C_n] [3–6] may further induce novel phenomena in binary mixtures by altering the subtle energy-entropy balance of the bulk. The bulk properties of such mixtures have been the subject of much interest [7] since the alkanes exist as mixtures in most "real-world" situations.

We have extensively studied two families of alkane mixtures, C_{20}-$C_{20+\Delta n}$ and $C_{36-\Delta n}$-C_{36}, where Δn ranges from 2 to 10. As for pure alkanes, a crystalline surface layer is found to form abruptly at T_s, *above* the bulk freezing temperature T_f. The Δn dependence of the surface phase behavior is found to be very similar for both families. As typical examples of small and large Δn behaviors, we present here results for two mixture series C_{30}-C_{36} and C_{26}-C_{36}.

Vigorously stirred molten mixtures of commercial alkanes of purity $\geq 99\%$ were poured onto a substrate mounted in a temperature-regulated cell. The free surfaces of the mixtures were studied by x-ray reflectivity (XR), x-ray grazing incidence diffraction (GID), and surface tension (ST) measurements. XR yields information on the electron density profile normal to the surface [8]. GID measurements provide information on the structure of a film within the surface plane [9]. The orientation of the molecular chains is obtained from the Bragg rods [9], i.e., the surface-normal dependence of the scattered intensity at the position of each in-plane GID peak. The ST measurements, using the Wilhelmy plate method [6,10], provide information on the excess free energy of the molecules at the surface over those in the bulk. The formation of the layer at T_s is seen as a sharp change from negative to positive slope in the surface tension $\gamma(T)$.

The measured XR for pure C_{30} and C_{36} and their equal volume mixture is shown in Fig. 1. At $T > T_s$ (curve d),

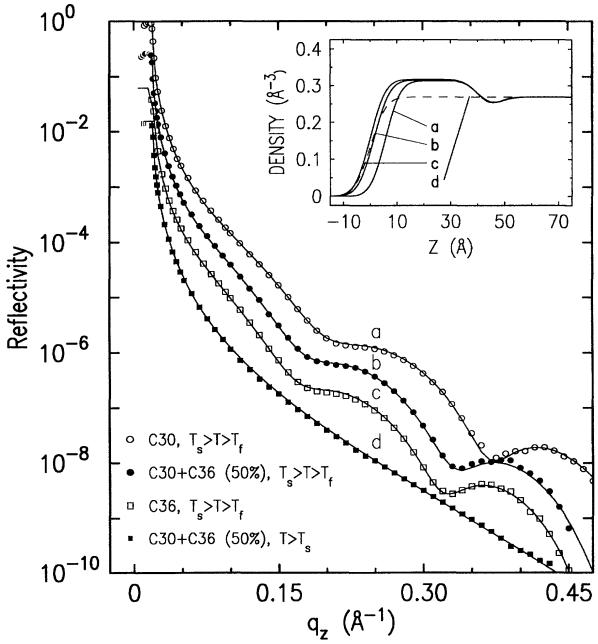

FIG. 1. X-ray reflectivities from the free surface of molten n alkanes C_{30}, C_{36}, and their 1:1 mixture in their surface crystalline phase ($T_s > T > T_f$), and from that of the 1:1 mixture in the surface liquid phase ($T > T_s$). The reflectivities are each shifted by a factor of 4 for clarity. The solid lines are fits corresponding to the density profiles in the inset.

 0031-9007/95/75(7)/1332(4)$06.00

when no surface layer is present, a monotonic falloff with q_z, typical of an isotropic liquid surface [11], is seen for all samples. At lower temperatures $T_f < T < T_s$ $(a-c)$, the XR curves for all three samples exhibit pronounced modulations, indicating the existence of a surface layer with an electron density different from that of the bulk. The different modulation periods results from different average surface layer thicknesses D. The XR data were fitted using a model assuming a layered interface consisting of a slab of higher electron density [representing the ordered $(CH_2)_{n-2}$ chains], and a lower density depletion zone at the layer-liquid interface (corresponding to the less dense CH_3 groups). The fit yields the density profiles shown in the inset. A 15% increase in the density of the surface layer over that of the liquid bulk is found for all mixtures. Note that D for the C_{30}-C_{36} mixture is intermediate between those for the two pure materials. We show in Fig. 2(a) that the average D varies continuously and monotonically with ϕ^l_{30} (the volume fraction of C_{30} in the bulk liquid), between those of pure C_{30} and C_{36}, implying a continuous change in the composition of the surface layer. A similar variation is found for the difference $\Delta(d\gamma/dT)$ in the slopes of the surface tension $\gamma(T)$ below and above T_s, shown in Fig. 2(b), supporting the same conclusion.

By contrast, the C_{26}-C_{36} mixtures exhibit a dramatically different surface behavior. D shows *discontinuous* behavior with ϕ^l_{26}, as seen in Fig. 2(c). For $\phi^l_{26} > 80\%$ and $\phi^l_{26} < 40\%$, D are those of pure C_{26} and C_{36}, respectively. In both cases the surface crystalline layer appears to consist of a single component: either C_{26} or C_{36}. For a range of ϕ^l_{26} between 70% and 80% no surface freezing is observed. Finally, for $40\% < \phi^l_{26} < 70\%$, a new surface phase appears, in which D is even slightly larger than that for pure C_{36}. The surface tension results, summarized in Fig. 2(d), also show clearly these four surface phases. Discrete $\Delta(d\gamma/dT)$ values, very close to those of pure C_{36} and C_{26} are observed for $\phi^l_{26} < 40\%$ and $\phi^l_{26} > 80\%$, respectively. Note that the biggest slope change is for the new, anomalous-D phase.

Another novel effect is observed for a concentration range of a few percent straddling the phase boundary at $\phi^l_{26} \approx 40\%$ in C_{26}-C_{36} mixtures. For all phases, at any fixed ϕ, only a single crystalline surface phase is observed as the temperature is lowered from T_s to T_f. By contrast, in this range it was found possible to effect a transition between the usual and new surface phases by varying the temperature. This is clearly seen by measuring the reflectivity at a fixed q_z, as shown in Fig. 3, where the formation of the ordinary C_{36} surface crystalline layer [4] is marked by an abrupt jump of intensity at $T_s \approx 70.0$°C. Another jump at $T \approx 69.0$°C marks the transition to the new surface structure, which persists down to $T_f \approx 68.5$°C. The surface tension measurements in the same figure also show these transitions. The first change of slope at 70.0°C marks the first order liquid-to-crystalline surface phase transition [6]. Its magnitude is roughly that expected from bulk data [12] for the entropy change upon a liquid-to-rotator phase transition in a monolayer. The second slope change at $T \approx 69.0$°C, marks the transition to the new, anomalous-D phase discussed above. Its magnitude is close to the entropy change observed at bulk rotator-to-crystal transitions, where the rotational degrees of freedom freeze out [12]. This unique surface crystalline structure can appear because the bulk T_f is much depressed here as compared to pure C_{36}.

X-ray GID and Bragg rod measurements show that except for the new surface phase the structure of the

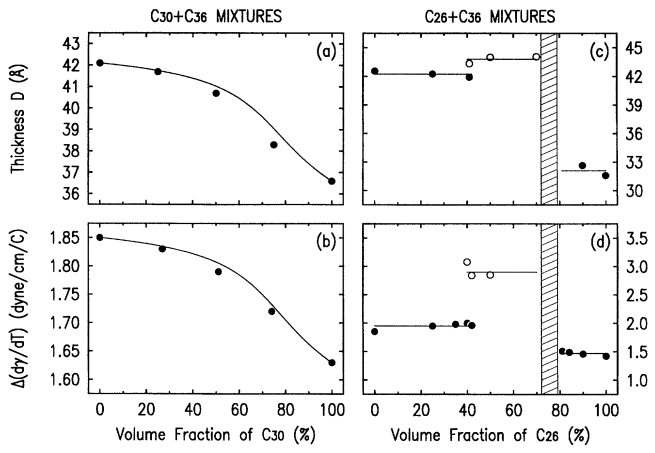

FIG. 2. For the C_{30}-C_{36} mixture series, (a) the thickness of the crystalline surface layer, (b) the slope difference of the surface tension between the surface crystalline and liquid phases. The solid lines are based on the surface crystalline compositions calculated according to Eqs. (1) and (2). (c) and (d) are the corresponding plots for the C_{26}-C_{36} mixtures. The open circles in (c) and (d) denote the new surface phase. Surface freezing is absent in the shaded region.

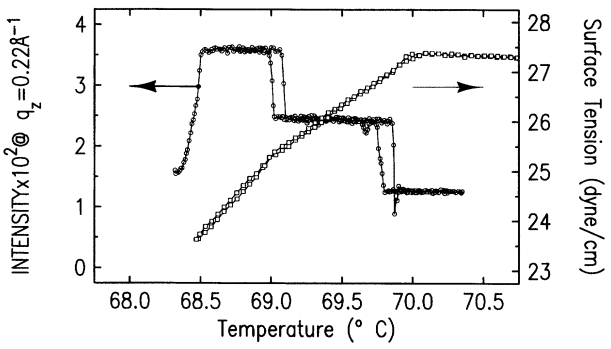

FIG. 3. The reflected intensity at $q_z = 0.22$ Å^{-1} for a C_{26}-C_{36} mixture with $\phi^l_{26} = 41\%$ and the surface tension of another sample with similar compositions. The formation of the crystalline surface layer at $T_s \approx 70$°C and the transition to a new surface crystalline structure at $T_n \approx 69$°C are clearly seen as jumps in the reflected intensity and slope changes in the surface tension. At bulk freezing $T_f \approx 68.4$°C, the surface becomes macroscopically rough and the reflected intensity drops considerably.

surface layer in mixtures is similar to that of pure alkanes [5]: hexagonal packing, with vertical molecules for $n < 30$ and tilted towards nearest neighbors for $n \geq 30$. The tilt angle increases with n and reaches 18° for C_{36}. GID peak widths are resolution limited for all samples, indicating crystalline coherence lengths $\geq$1000 Å. For the new phase, the Bragg rod data suggest that the tilt angle has decreased from 18° to only 13.5°, thus increasing D, and the tilt direction has changed from nearest to next-nearest neighbors. This structural transition is first order, whether induced by concentration or temperature variation.

The dichotomy between large and small Δn behavior extends also to the measured ϕ dependence of T_f and T_s, shown in Fig. 4. For small Δn [Fig. 4(b)] both vary in parallel, so that $\Delta T = T_s - T_f$, the existence range of the crystalline surface phase, is practically constant [Fig. 4(a)]. For large Δn, however, the two temperatures vary differently [Fig. 4(d)] and large variations in ΔT with concentration result [Fig. 4(c)].

The features observed in our measurements can be accounted for by the general thermodynamics of binary mixtures [13], based on the properties of the pure components [6]. The free energy $F^{i,j}$ of a mixture of $N^{i,j}$ moles of C_n molecules and $M^{i,j}$ moles of C_m molecules, where $i = l, c$ (liquid, crystalline) and $j = b, s$ (bulk, surface), can be written generally as [14,15]

$$F = Nf_n + Mf_m + k_bT[N\ln(\phi) + M\ln(1 - \phi)] + k_bT\chi(N + M)\phi(1 - \phi), \quad (1)$$

where the indices i, j were dropped for clarity. Here $f_{n,m} = \varepsilon_{n,m} - TS_{n,m}$ is the free energy of a $C_{n,m}$ molecule in a pure melt (S is the entropy, ϵ the internal energy), the logarithmic term accounts for the entropy of mixing, and the last term accounts for the repulsion due to the mismatch of the chain lengths of the two species [14–18]. In the liquid phase, $\phi = nN/(nN + mM)$ is the volume fraction, the repulsive interaction is negligible ($\chi \approx 0$), so that the mixing entropy is dominant [12]. In the crystalline phase $\phi = N/(N + M)$ is the mole fraction. Since now all molecules are aligned parallel and chains of different lengths are packed at random into layers, the repulsive interaction ($\chi > 0$) due to chain mismatch is considerable. This repulsive interaction favors phase separation, whereas the entropy favors random mixing [13]. For small mismatch $\chi < 2$, the mixing entropy is dominant and a mixed homogeneous crystalline phase of a definite composition forms. For large mismatch $\chi > 2$, however, the repulsive interaction dominates and phase separation into C_n-rich and C_m-rich domains occurs [16]. The interaction coefficient χ must increase with the chain mismatch [12,17,18]. Based on symmetry considerations, it is expected to be proportional to $(\Delta n/\bar{n})^2$, with $\bar{n} = (n + m)/2$.

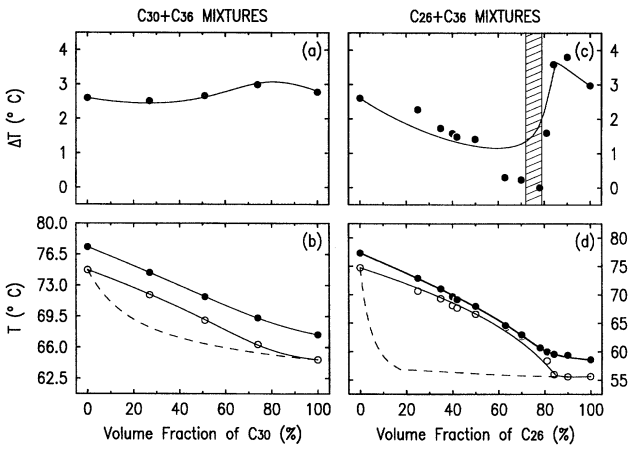

FIG. 4. (a),(c) Existence range $\Delta T = T_s - T_f$ for the surface crystalline phase, (b),(d) and surface T_s (•) and bulk T_f (○) freezing temperatures for the mixtures, respectively. The solid lines in (b),(d) are the fits based on Eqs. (1) and (2). The dashed lines are the calculated lower boundaries of the bulk liquid-solid coexistence regions. Shading marks the range where surface freezing is absent, separating the C_{26}-rich from the C_{36}-rich surface crystalline phases.

The bulk solid-liquid coexistence requires that the chemical potentials ($\partial F/\partial N$ and $\partial F/\partial M$) for each component be equal in the two phases. This yields two equations from which the coexistence temperature T_f and the crystalline concentration $\phi^{c,b}$ at coexistence are solved in terms of the liquid concentration $\phi^{l,b}$, the pure component properties, and the interaction coefficient χ. χ was obtained by fitting these analytic solutions to the measured bulk T_f as a function of $\phi^{l,b}$ [solid lines in Figs. 4(b) and 4(d)]. In turn, $\phi^{c,b}$ was calculated as a function of $\phi^{l,b}$ based on the fitted χ. This $\phi^{c,b}$ vs $\phi^{l,b}$ relation determines the lower boundary of the bulk liquid-solid coexistence region [dashed lines in Figs. 4(b) and 4(d)]. We find that the bulk interaction parameter is well fitted by $\chi^b \approx 18(\Delta n/\bar{n})^{1.8}$ for all the mixtures studied, consistent with the expectations in the last paragraph. For small Δn where $\chi < 2$, $\phi^{c,b}$ varies continuously with $\phi^{l,b}$. Here the crystalline phase is always richer in the longer chain species than the liquid phase. For large Δn where $\chi > 2$, $\phi^{c,b}$ is almost everywhere close in composition to one of the pure single components; i.e., the long and short chains phase separate.

Similar analysis is applied to the surface solid-liquid coexistence. However, here we need to relate the surface liquid concentration $\phi^{l,s}$ to the experimental control parameter—the bulk liquid concentration $\phi^{l,b}$. Invoking the equality of the chemical potentials of the surface and bulk liquids we can write [14]

$$\frac{\phi^{l,s}}{\phi^{l,b}} = \frac{1 - \phi^{l,s}}{1 - \phi^{l,b}} \exp\left(- \frac{(\gamma_n - \gamma_m)A}{k_bT} + \frac{(n - m)^2}{nm}(\phi^{l,s} - \phi^{l,b}) \right), \quad (2)$$

where $\gamma_{n,m}$ are the surface tensions of pure $C_{n,m}$ melts and A is the area per molecule. At a given temperature,

γ_n decreases with n as $\gamma_n = a(T) - bn^{-2/3}$, with $b = 65.4$ dyn/cm [6,12]. Thus the surface tension term in Eq. (2) drives a slight surface enrichment of the shorter component in the liquid surface phase. However, since the difference is small and continuous, the general phase behavior is very close to that of the bulk. The solid lines in Figs. 4(b) and 4(d) fit the data very well, yielding a surface interaction parameter $\chi^s \approx 14(\Delta n/\bar{n})^2$, close to the bulk χ^b obtained above. We obtain $A \approx 110$ and 70 Å^2 for the $C_{36-\Delta n}$-C_{36} and C_{20}-$C_{20+\Delta n}$ series, respectively. While this clearly reflects changes in packing efficiency, the exact interpretation of these values is unclear. Using the crystalline surface compositions $\phi^{c,s}$ obtained to interpolate linearly between the layer thicknesses and slope changes of the pure materials yields the solid lines in Figs. 2(a) and 2(b), in reasonable agreement with the measurements.

In essence, the discussion above indicates that *when both bulk and surface are liquid* the surface composition is determined by that of the bulk through the equality of the bulk (μ^b) and surface (μ^s) chemical potentials of each component. The bulk and surface differ in composition since μ^s includes a surface tension contribution. The difference $\gamma_n - \gamma_m$ determines, through Eq. (2), the (small) deviation of the surface composition from that of the bulk. The bulk (surface) composition *in the solid phase,* is determined, again, by the requirement of equal chemical potentials for each component at coexistence T_f (T_s). Since the mismatch term is nonzero in the solid but ≈ 0 in the liquid, it has a strong influence on the composition of the solid, and, in particular, on whether or not phase separation occurs. As the mismatch energies, liquid compositions, and pure component coexistence temperatures are different at the surface and the bulk, the resultant mixture coexistence temperatures and solid compositions will also differ for the bulk and surface. To conclude then, the liquid bulk composition and pure component properties control the phase behavior at the surface, and the surface tension difference $\gamma_n - \gamma_m$ has only a minor influence.

We believe that this is the first molecular-resolution study of the phase diagram of the free surface of a liquid binary mixture. In addition to the novel surface freezing phenomenon seen in the pure components, the bidisperse n alkanes studied here exhibit a new surface phase and a phase transition between two distinct crystalline structures. A simple thermodynamic model, where the mixing entropy is balanced by a repulsive interaction due to chain length mismatch, Δn, was found to account quantitatively for the overall phase behavior, including the transition temperatures and the surface and bulk compositions. Δn was found to tune the system between two dramatically different behaviors. Further studies, over a larger range of chain lengths and on different materials are in progress to elucidate the surface phase behavior in chain molecules and its relations with the phase behavior of the bulk.

This work was supported in part by the U.S.-Israel Binational Science Foundation, Jerusalem, Exxon Education Foundation and UIUC MRL via DOE Grant No. DEFG02-91ER 45439. BNL is supported by the Division of Materials Research, DOE under Contract No. DE-AC02-76CH00016.

[1] T. Getta and S. Dietrich, Phys. Rev. E **47**, 1856 (1993), and references therein.

[2] P. G. deGennes, Rev. Mod. Phys. **57**, 827 (1985); A. J. Liu and M. E. Fisher, Phys. Rev. A **40**, 7202 (1989); J. W. Schmidt and M. R. Moldover, J. Chem. Phys. **99**, 582 (1993); B. M. Law, Phys. Rev. Lett. **69**, 1781 (1992); H. Kellay, D. Bonn, and J. Meunier, Phys. Rev. Lett. **71**, 2607 (1993).

[3] J. C. Earnshaw and C. J. Hughes, Phys. Rev. A **46**, R4494 (1992).

[4] X. Z. Wu, E. B. Sirota, S. K. Sinha, B. M. Ocko, and M. Deutsch, Phys. Rev. Lett. **70**, 958 (1993).

[5] X. Z. Wu, M. Deutsch, B. M. Ocko, E. B. Sirota, and S. K. Sinha (to be published).

[6] X. Z. Wu, B. M. Ocko, E. B. Sirota, S. K. Sinha, M. Deutsch, B. H. Cao, and M. W. Kim, Science **261**, 1018 (1993).

[7] E. B. Sirota, H. E. King, Jr., H. H. Shao, and D. M. Singer, J. Phys. Chem. **99**, 798 (1995), and references therein.

[8] J. Als-Nielsen, F. Christensen, and P. S. Pershan, Phys. Rev. Lett. **48**, 1107 (1982); T. P. Russell, Mater. Sci. Rep. **5**, 171 (1990).

[9] J. Als-Nielsen and K. Kjaer, in *Phase Transitions in Soft Condensed Matter,* edited by T. Riste and D. Sherrington (Plenum, New York, 1989); D. K. Schwartz, M. L. Schlossman, and P. S. Pershan, J. Chem. Phys. **96**, 2356 (1991).

[10] G. L. Gaines, *Insoluble Monolayers at the Liquid Gas Interface* (Wiley, New York, 1966).

[11] A. Braslau, P. S. Pershan, G. Swislow, B. M. Ocko, and J. Als-Nielsen, Phys. Rev. A **38**, 2457 (1988); M. K. Sanyal, S. K. Sinha, K. G. Huang, and B. M. Ocko, Phys. Rev. Lett. **66**, 628 (1991); B. M. Ocko, X. Z. Wu, E. B. Sirota, S. K. Sinha, and M. Deutsch, Phys. Rev. Lett. **72**, 242 (1994).

[12] D. M. Small, *The Physical Chemistry of Lipids* (Plenum, New York, 1986).

[13] L. E. Reichl, *A Modern Course in Statistical Physics* (University of Texas, Arlington, 1980).

[14] R. Defay, I. Prigogine, A. Bellemans, and D. H. Everett, *Surface Tension and Adsorption* (Wiley, New York, 1966).

[15] P. Flory, *Principles of Polymer Chemistry* (Cornell, Ithaca, 1953).

[16] R. R. Matheson, Jr. and P. Smith, Polymer **26**, 289 (1985).

[17] J. I. Lauritzen, Jr. and E. Passaglia, J. Res. Natl. Bur. Stand. Sect. A **71**, 261 (1967); J. Chem. Phys. **45**, 4444 (1966).

[18] D. H. Bonsor and D. Bloor, J. Mater. Sci. **12**, 1559 (1977).